Full Dimensional Ab Initio Dynamics Calculations of Electron Capture Processes of the H_4^+ Ion

Hiroto Tachikawa*

Division of Molecular Chemistry, Graduate School of Engineering, Hokkaido University, Sapporo 060-8628, Japan

Received: February 9, 2000; In Final Form: May 24, 2000

Electron capture processes of H_4^+, that is, $H_4^+ + e^- \rightarrow H_2 + H_2$, have been studied by means of direct ab initio dynamics calculations to elucidate the reaction mechanism. The ab initio molecular orbital calculations showed that the structure of H_4^+ is flexible and its intermolecular motion $H-H_3^+$ is composed of a low-frequency mode. The H_4^+ ion has a wide Franck−Condon (FC) region for the direction of the low-frequency mode. In dynamics calculations, we assumed that all trajectories run on the ground state of H_4 and that auto-ionization does not take place once the H_4^+ ion captures an electron. A total of 120 trajectories were run from the initial geometries of H_4 chosen from the FC region. Each trajectory gave two kinds of hydrogen molecules: a vibrationally excited hydrogen molecule (hot-H_2) and a vibrationally ground-state H_2 (cold-H_2). The vibrational quantum number of cold-H_2 was populated only in $v = 0$, whereas that of hot-H_2 was widely distributed in $v = 4-8$. About 30% of the total available energy was partitioned into the relative translational mode between hot-H_2 and cold-H_2. The reaction mechanism of the electron capture processes of H_4^+ is discussed on the basis of the theoretical results.

1. Introduction

Ion clusters of hydrogen atoms (H_n^+) and hydrogen molecules (H_{2n}^+) are important species in interstellar cloud.[1−11] Among them, H_3^+ ion plays an important role as a proton donor and an electron acceptor in chemical reaction with neutral molecule and electron in a dark cloud, respectively. Studying H_3^+ provides information on detailed reaction dynamics in the cloud. The positive ion H_4^+, composed of an even hydrogen atom, has been shown both computationally[12−14] and experimentally[15] to be a stable species. Borkman et al. carried out accurate ab initio calculations of H_4^+ systems.[16−18] They showed that H_4^+ has a planar C_{2v} geometry consisting of a triangle of three H atoms with a fourth H bonded to one vertex. Namely, H_4^+ is composed of H_3^+ and H atom, which is expressed by H_3^+-H. The ab initio molecular orbital (MO) calculations showed that the triangular part of H_4^+ contains three strong H−H bonds with high-frequency ring-stretching vibrations similar to the well-known H_3^+ ion. The fourth H atom in H_4^+ is bound weakly to H_3^+, so that the H_3^+-H stretching vibration displays a lower frequency. The best calculation provided the spectroscopic constants ($D_e = 4.8$ kcal/mol and $w_e = 610$ cm^{-1}).[16−18] H_4^+ was detected by mass spectrometry in 1984.[15]

Recently, there has been interest in charge neutralization reactions of small ions containing hydrogen (e.g., $H_3^+ + e^-$ and $H_4^+ + e^-$).[19,20] Pan and Borkman investigated the electron capture process of H_4^+, $H_4^+ + e^- \rightleftharpoons H_4^*$, using ab initio MO calculations. They calculated potential energy surfaces for the dissociation between H_2 molecules and found that H_4^*, formed by the electron capture by H_4^+, decomposed into the hydrogen molecules $H_4^* \rightarrow H_2 + H_2$. Also, they predicted that the product hydrogen molecules are composed of two kinds of hydrogen molecule, that is, vibrationally hot-H_2 and cold-H_2. However, they did not obtain detailed features because they did not apply a dynamics calculation.

In this article, a full dimensional direct ab initio dynamics calculation is applied to the electron capture processes of H_4^+

$$H_4^+ + e^- \rightarrow H_4^* \qquad (1)$$

to elucidate detailed reaction dynamics. In particular, we focus our attention on the product states of the vibrational−rotational states of H_2 and relative translational energy between the products. In this study, we assumed that the reaction of H_4 proceeds on the ground-state potential energy surface, once an electron is captured by H_4^+. The dynamics on the Rydberg state surface of H_4 were not considered throughout.

2. Computational Method

In general, the classical trajectory is performed on an analytically fitted potential energy surface as previously performed by several groups[21] and by us.[22] However, it is not appropriate to predetermine the reaction surfaces of the present systems because of the numerous degrees of freedom ($3N - 6 = 6$, where N is number of atoms in the system). Therefore, in this study, we applied the direct ab initio trajectory calculation with all degrees of freedom. The details of the direct dynamics method are described elsewhere.[23]

In the direct ab initio dynamics calculation, we used the 6-311G(d,p) basis set for the electron capture process of H_4^+ throughout. First, the HF/6-311G(d,p) optimized geometry of H_4^+ was chosen as an initial structure. Second, several initial geometries were selected from the Franck−Condon (FC) region, and then the trajectories were calculated. We considered the intermolecular stretching mode ($v = 0$) between H and H_3^+ calculated at the HF/6-311G(d,p) level. The equations of motion for n atoms in a reaction system are given by

* hiroto@eng.hokudai.ac.jp.

10.1021/jp0005219 CCC: $19.00
Published on Web 07/28/2000

$$\frac{dQ_j}{dt} = \frac{\partial H}{\partial P_j} \quad (2)$$

$$\frac{\partial P_j}{\partial t} = -\frac{\partial H}{\partial Q_j} = -\frac{\partial U}{\partial Q_j} \quad (3)$$

where $j = 1-3N$, H is classical Hamiltonian, Q_j is the Cartesian coordinate of the jth mode, and P_j is the conjugated momentum. These equations were solved numerically by the Runge−Kutta method. No symmetry restriction was applied to the calculation of the gradients in the Runge−Kutta method. The time step size was 0.10 fs, and a total of 10 000 steps was calculated for each dynamics calculation. The drift of the total energy was confirmed to be less than 0.1% throughout all steps in the trajectory. The momentum of the center of mass and the angular momentum around the center of mass were also confirmed to retain at the initial value of zero. Static ab initio MO calculations were performed using the GAUSSIAN-94 program.[24]

3. Results

A. Structure and Electronic States of H_4^+. First, the structure of H_4^+ was optimized by the energy gradient method at the HF/6-311G(d,p) level. The H_4^+ ion has a C_{2v} structure constructed by a triangular skeleton of H_3 and a hydrogen atom in a corner of the triangular part of H_3. The schematic illustration of the structure of H_4^+ is given in Figure 1. The optimized parameters of H_4^+ calculated were $r_1 = 1.6097$ Å, $r_2 = 0.9004$ Å, $r_3 = 0.8437$ Å, $\theta = 55.9°$, and $\phi = 152.1°$. The numerical values of H_4^+ were in good agreement with those obtained by Pan and Borkman.[14] To elucidate the electronic states of H_4^+, the charge on each atom was calculated at the MP4SDQ/6-311G(d,p)//HF/6-311G(d,p) level. The results are summarized in Table 1. In the H_4^+ ion, the positive charge was delocalized mainly over the triangular part composed of the H_3 moiety of H_4^+, whereas the charge on the hydrogen H(1) was close to zero (+0.13e). Instead, an unpaired electron was almost localized on H(1). The binding energies of H to H_3^+ were calculated to be 3.0 kcal/mol (HF level) and 4.2 kcal/mol (MP4SDQ level), which are in reasonable agreement with the numeric values obtained previously.[14,16−18] The agreement revealed that the dynamics calculations at the HF/6-311G(d,p) level would give reasonable features of the reaction dynamics.

Second, the harmonic vibrational frequencies of H_4^+ were calculated at the HF/6-311G(d,p) and MP4SDQ/6-311G(d,p) levels. The numeric values are given in Table 2. The HF calculation gave reasonable values for the vibrational frequencies of H_4^+. The highest frequency (3523 cm^{-1}) corresponded to the ν_1-mode of free H_3^+: a symmetric deformation of triangular structure of H_3. The degenerated ν_2-mode of free H_3^+ splits into the b_2- and a_1-modes in H_4^+ by the interaction with the H(1) atom. The smallest frequency (480 cm^{-1}) corresponds to the stretching mode between H(1) and H(2). This mode moves along the r_1 direction. Mode 5 (b_2, 532 cm^{-1}) is composed of a bending mode of H(1)−H(2)−H(3), where H(1) moves along the ϕ-angle direction on the molecular plane. These numeric values indicate strongly that the structure of H_4^+ is nonrigid and that H_4^+ has a wide FC region mainly for the r_1 direction. In the trajectory calculation, therefore, we considered the electron capture processes from the wide FC region with sampling of the starting points.

B. Dynamics of the Electron Capture by H_4^+. As mentioned above, the H_4^+ ion has a wide FC region mainly for the r_1 direction. Therefore, we sampled 120 geometries of H_4^+ on the FC region as initial structures. In this study, we considered only FC for the vibrational ground state ($v = 0$). One-dimensional Gaussian distribution along the r_1 direction ($r_1 = 1.38-1.84$ Å, and the center of the potential curve is located at $r_1 = 1.61$ Å) was assumed as distribution of sampling points in the FC region. The ϕ-angle was randomly distributed as $\phi = 152.1 \pm 1.0°$. Therefore, the initial structure of H_4 was near-C_{2v}.

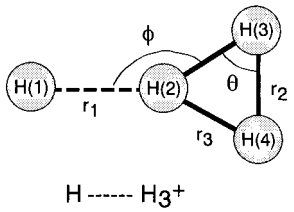

Figure 1. Geometrical parameters and schematic structure of the reaction system of H_4^+ and H_4.

TABLE 1: Charge on Each Atom of H_4^+ Calculated at the HF/6-311G(d,p) and MP4SDQ/6-311G(d,p)//HF/6-311G(d,p) Levels of Theory[a]

atom	HF	MP4SDQ
H(1)	0.128 (0.875)	0.134 (0.867)
H(2)	0.244 (0.080)	0.236 (0.095)
H(3)	0.314 (0.022)	0.315 (0.019)

[a] Spin densities are given in parentheses. C_{2v} symmetry is assumed.

TABLE 2: Harmonic Vibrational Frequencies (in cm^{-1}) of H_4^+ Calculated at the HF/6-311G(d,p) and MP4SDQ/6-311G(d,p) Levels of Theory

mode	sym.	HF	MP4SDQ[a]	description
1	a_1	3523	3480	ν_1 mode of H_3^+
2	b_2	2620	2254	ν_2 mode of H_3^+
3	a_1	2590	2219	ν_2 mode of H_3^+
4	b_1	715	877	H(1) bend (out of plane)
5	b_2	532	682	H(1)−H(2)−H(3) and −H(4) bend (in-plane)
6	a_1	480	643	H(1)−H(2) stretch.

[a] Optimized parameters obtained at the MP4SDQ/6-311G(d,p) level are $r_1 = 1.3792$ Å, $r_2 = 0.9444$ Å, $r_3 = 0.8382$ Å, $\theta = 63.7°$, and $\phi = 153.7°$.

Sample Trajectory. The result of the dynamics calculation for a sample trajectory is given in Figure 2. For this trajectory, the geometry of H_4* at the starting point corresponds to the optimized structure of H_4^+; namely, the potential energy surface of H_4^+ is changed vertically by the electron capture to that of the neutral H_4 without structural change. Figure 2A shows the potential energy of the reaction system calculated as a function of reaction time, and distances and angles are plotted in parts B, C, and D of Figure 2. Zero level in Figure 2A corresponds to the total energy at the point of the vertical electron capture of H_4^+ (i.e, $[H_4]_{ver}$). After starting the trajectory calculation, the potential energy decreased suddenly to −5 eV within a very short time (about 5 fs). Within this period, the distance (r_1) decreased from 1.6 to 0.4 Å, meaning that the H(2) atom of triangular part H_3^+ approaches the H(1) atom. H(2) collided with H(1) at time = 5.0 fs, and the H(1)−H(2) molecule was newly formed. After that, the H−H stretching mode of the hydrogen molecule formed by the collision was strongly vibrated; the amplitude was as large as 1.20 Å ($r_1 = 0.42-1.62$ Å). On the other hand, the amplitude of the H−H stretching mode of the H(3)−H(4) molecule was 0.116 Å ($r_2 = 0.68-0.797$ Å), which corresponds to the vibrational ground state of the H_2 molecule. These results indicate that two kinds of hydrogen molecules are formed by the electron capture by H_4^+;

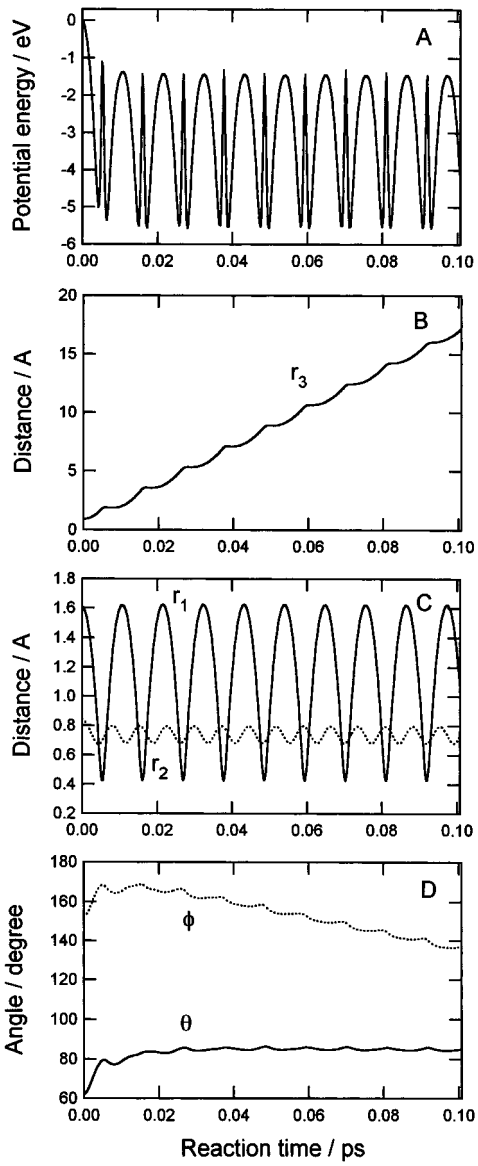

Figure 2. A typical trajectory for the H_4 molecule formed by the vertical electron capture by H_4^+ plotted as a function of reaction time. (A) The potential energy of the reaction system; (B) the intermolecular distance between the hydrogen molecules r_3; (C) intramolecular distances r_1 and r_2; and (D) angles (θ and ϕ) versus time. The direct ab initio dynamics calculation was performed at the HF/6-311G(d,p) level.

these are vibrational cold-H_2 and hot-H_2. The intermolecular distance between cold-H_2 and hot-H_2 (denoted by r_3) increases linearly from 3.644 to 16.98 Å within 0.10 ps, meaning that the hydrogen molecules leave each other with a relative translational energy of 33.2 kcal/mol, which corresponds to 26% of the total available energy. The angles (θ and ϕ) are hardly varied, meaning that both cold-H_2 and hot-H_2 molecules are in a rotational ground state.

Snapshots. Snapshots of the conformation of the H_4 system are illustrated in Figure 3. Before the electron capture of H_4^+, the H(1) atom interacts weakly with the H(2) in the trianglar part of H_3^+. After the vertical electron capture by H_4^+, the interaction between H(1) and H(2) becomes strongly attractive, whereas the interaction between H(2) and H(3) or H(4) becomes strongly repulsive. At 5 fs, H(2) moves rapidly and collides with H(1). After that, H(2) is recoiled by H(1), and then H(1) leaves from H(2). However, H(1) is not fully separated from H(2) because of a strong attractive interaction between H(1)

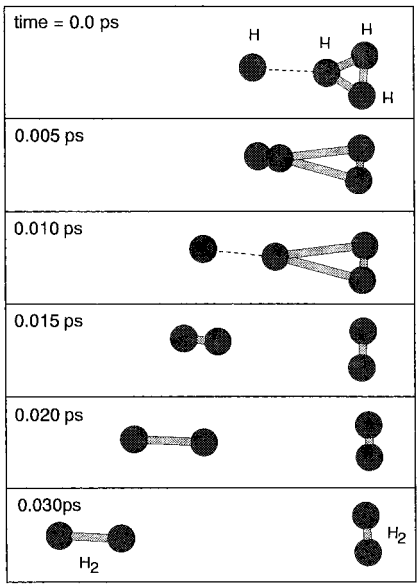

Figure 3. Snapshots for configurations of H_4 after the vertical electron capture by H_4^+ calculated as a function of time. The direct ab initio dynamics calculation was performed out at the HF/6-311G(d,p) level.

and H(2). This strong collision between H(1) and H(2) causes vibrational excitation of the H−H stretching mode of the H(1)−H(2) molecule. The mode of H(1)−H(2) is thus highly excited, whereas that of H(2)−H(3) is in a vibrational ground state. The H(1)−H(2) molecule is separated from the H(3)−H(4) molecule because of the strong repulsive interaction between H_2 and H_2.

C. Population of Vibrational Quantum Number of the Product H_2 Molecules. A total of 120 trajectories are calculated from the different initial geometrical configurations on the FC region. Populations of the product internal states and the relative translational energy are given in Figure 4. Figure 4A clearly shows that the population of the vibrational quantum number of the H−H stretching mode is bimodal: one is populated only in $v = 0$, whereas the second is distributed widely from $v = 4$ to 8, with a peak of $v = 6$. The population of $v = 0$ is composed of the H(3)−H(4) molecule, whereas it is higher vibrational quantum number is the H(1)−H(2) molecule. It is therefore concluded that the electron capture by H_4^+ gives two kinds of hydrogen molecules as products: one is in the vibrational ground state, and the other is in the vibrational excited state. These correspond to cold-H_2 and hot-H_2. The population of vibrational states for hot-H_2 is widely distributed, whereas the population of vibrational states for cold-H_2 is only in $v = 0$. The product rotational quantum number of the hydrogen molecules obtained was only $J = 0$.

Population of the relative translational energy between the hydrogen molecules, formed by the electron capture by H_4^+, is given in Figure 4B. The energy is widely distributed from 25 to 50 kcal/mol with a peak at 33 kcal/mol.

D. Angle Dependence on the Dynamics. In section 3B, we calculated the trajectories from the near-C_{2v} structure of H_4. As mentioned in section 3A, the H_4^+ ion has another lower vibrational mode that corresponds to the bending mode of H(1)−H(2)−H(3) (i.e., deformation along the ϕ-angle). In this section, to elucidate angle dependence on the reaction dynamics of H_4, trajectories from the FC region for the ϕ-direction are calculated in the same manner. The vibrational frequency of the bending mode is calculated to 532 cm^{-1} as given in Table 2. The outer edge of the FC region is estimated by $\phi = 152 \pm 23°$ for $v = 0$. From the FC region, we selected five angles ($\phi = 155$, 160, 165, 170, and 175°), and then trajectories were calculated.

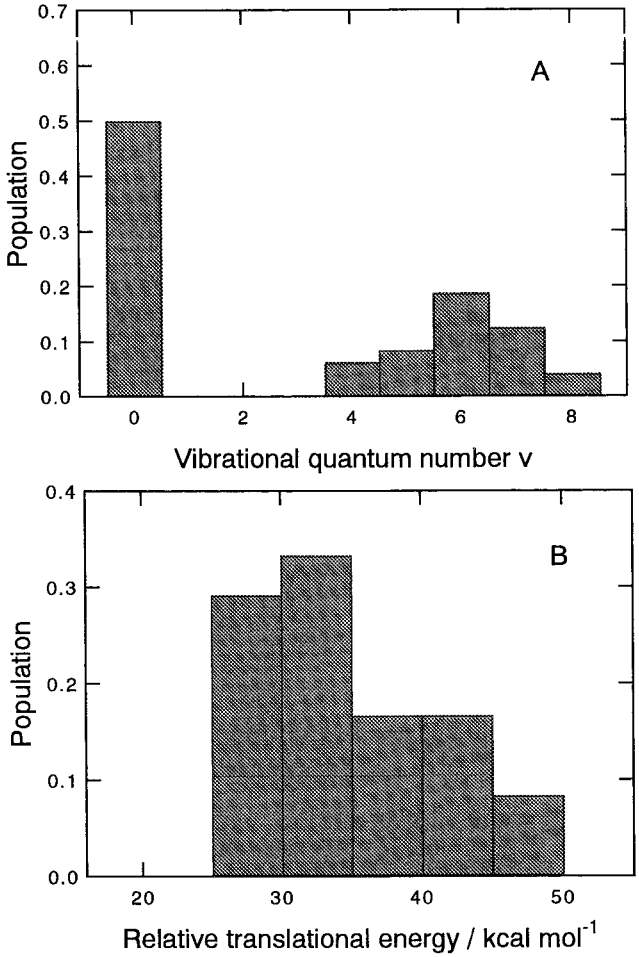

Figure 4. Populations of (A) vibrational quantum number of the product H_2 molecules and (B) relative translational energies between H_2 molecules formed by the electron capture by H_4^+.

Sample Trajectory. The result of the dynamics calculation for a sample trajectory is given in Figure 5. The geometry of H_4 at the starting point corresponds to that in the outer edge of FC region ($\phi = 175°$). The dynamics feature obtained for $\phi = 175°$ is similar to those of the near-C_{2v} structure. Therefore, we discuss briefly the reaction dynamics in this section. The potential energy of the reaction system calculated as a function of reaction time is plotted in Figure 5A. The potential energy decreases to -5 eV at time 5 fs, and then it vibrates in the range from -5.57 to -1.32 eV. The time dependence of r_3 indicates that the hydrogen molecule leaves rapidly from the other H_2 molecule after the electron capture. Figure 5C clearly indicates that the vibrational mode of the H(3)−H(4) molecule is in the ground state, whereas the other H_2 molecule is vibrationally hot. Time dependence of the angles (θ and ϕ) is plotted in Figure 5D. As shown in this figure, the angles are slightly different from those given in Figure 2D. At time zero, the angles (θ and ϕ) are 55.9 and 175°, respectively. After the electron capture of H_4^+, these angles decrease gradually and are close to zero at time 7 fs. This means that the rotation of the H(1)−H(2) molecule occurs after the electron capture of the H_4^+ ion with a bent structure. However, the rotational period is very long, meaning that the energy is hardly transferred into the rotational mode of H_2 even in the outer edge of the FC region.

Snapshots. Snapshots of the conformation of the H_4 system are illustrated in Figure 6. The hydrogen atom H(1) is located at $r_1 = 1.608$ Å and $\phi = 175.0°$ at time zero, meaning that the

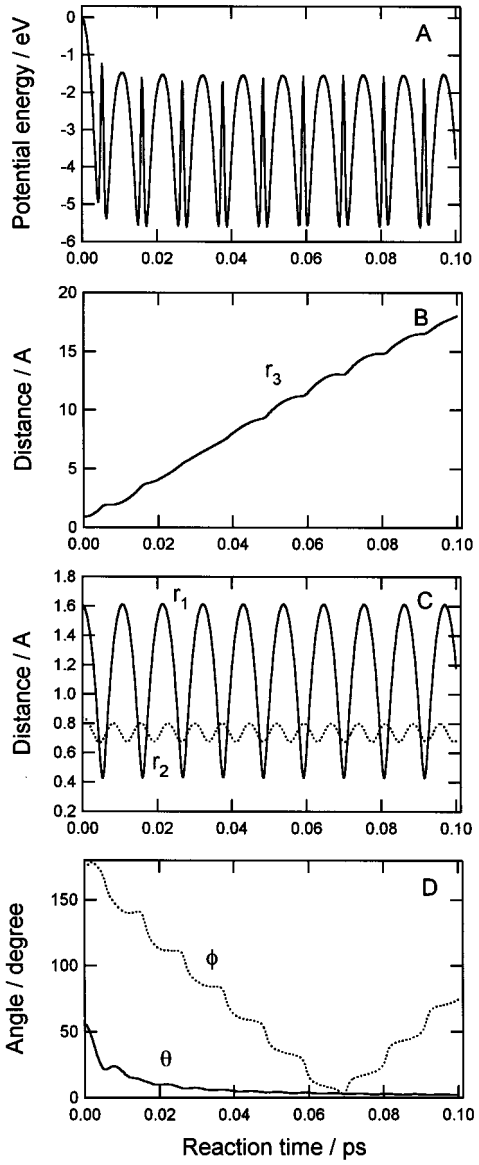

Figure 5. A trajectory for the H_4 molecule formed from the outer edge of the FC region for the ϕ-direction. (A) Potential energy of the reaction system; (B) intermolecular distance between the hydrogen molecules r_3, (C) intramolecular distances r_1 and r_2, and (D) angles (θ and ϕ) versus time. The direct ab initio dynamics calculation was performed at the HF/6-311G(d,p) level.

trajectory at the starting point is located in the outer edge of the FC region. The H(2) collides with the H(1) at time 5 fs, and two hydrogen molecules are formed. At this time, the bond distances r_1 and r_2 become 0.4725 and 1.8150 Å, respectively. The H(2)−H(3) distance is shortened from 0.8430 to 0.6747 Å within 5 fs. After the collision, the H(1)−H(2) distance is significantly elongated. ($r_1 = 1.5889$ Å at 10 fs, and the intermolecular distance r_2 is 2.1433 Å.) At 15 fs, the intermolecular distance becomes 3.2492 Å, and the interaction between the two hydrogen molecules becomes weaker. As clearly seen in Figure 6, the H(1)−H(2) molecule is rotated after the collision. However, the rotation period of the hydrogen molecule is very long; the rotational excitation of H_2 hardly occurs in the electron capture of the vibrationally ground-state H_4^+.

A total of five trajectories are calculated from the different initial geometrical configurations on the FC region. Relative translational and rotational energies of the products are summarized in Table 3. The relative translational energy (E_{tr}) increases with increasing angle (ϕ) and reaches a maximum at

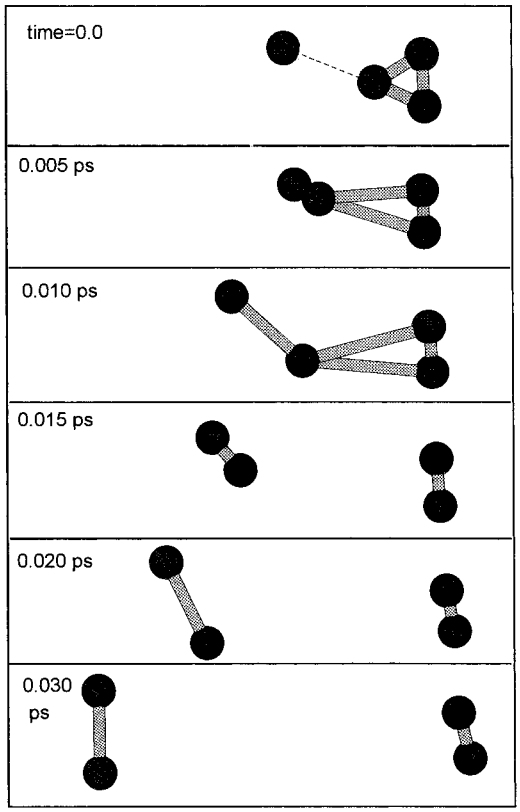

Figure 6. Snapshots for configurations of H_4 formed from the outer edge of FC region for ϕ-direction calculated as a function of time. The direct ab initio dynamics calculation was carried out at the HF/6-311G-(d,p) level.

TABLE 3: Angle Dependence on the Reaction Dynamics of Electron Capture by H_4^+ [a]

angle ϕ	E_{tr}	E_{rot}	comment
152.1	32.9	0.0	optimized structure
155.0	34.1	1.6	
160.0	36.4	3.4	
165.0	37.0	5.9	
170.0	35.1	10.9	
175.0	31.9	15.1	outer edge of FC region

[a] Initial ϕ-angle (in degrees), relative translational energy between product hydrogen molecules (E_{tr} in kcal mol^{-1}), and rotational energy of H(1)−H(2) (E_{rot} in cal mol^{-1}).

$\phi = 165°$. E_{tr} decreases gradually at larger angles. The translational energies in the maximum point and in the outer edge of FC region are calculated to be 37.0 and 31.9 kcal/mol, respectively. The rotational energy of H(1)−H(2) increases linearly with increasing angle ϕ. However, the magnitude is very small as shown in Table 3. The product rotational quantum number of the hydrogen molecules was obtained by only $J = 0$.

E. Trajectories from a Geometrical Configuration at Rydberg State. To elucidate the effect of the Rydberg state on the reaction dynamics, preliminary trajectory calculations from a geometrical configuration optimized for the Rydberg 2s state (the lowest Rydberg state) are run. The structure of H_4 at the lowest Rydberg state is optimized at the single excited configuration interaction (S-CI) method with a basis set 6-311G-(d,p)+Rydberg orbital.[14b] The calculated optimized parameters under C_{2v} symmetry are: $r_1 = 2.1206$ Å; $r_3 = 0.9194$ Å; $\phi = 93.1°$. The triangular structure of H_4^+ is largely deformed at the Rydberg state of H_4; the conformation of the H(2)−H(3)−H(4) skeleton is close to linear, and H(1) is located at a longer distance from H(2). Two trajectories are run from the structures with near-C_{2v} symmetry (we choose $\phi = 93.1 + 1.0°$ and $\phi = 93.1 + 2.0°$). The dynamics feature obtained is much different from that of the vertical electron capture to the ground-state H_4. After radiative transition from Rydberg-H_4 to the ground state, the hydrogen atoms H(2) and H(3) approach H(4) and H(1), respectively. In particular, the collision of H(3) with H(1) takes place strongly. Two kinds of the hydrogen molecules, H(1)−H(3) and H(2)−H(4), are formed as products. The former hydrogen molecule has a large vibrational energy corresponding to $v = 9$ or 10, which is higher than that of the vertical electron capture of H_4^+. The vibrational mode of the latter hydrogen molecule is in the ground state. The relative translational energy between the products is calculated to be 42 kcal/mol. Thus, the present dynamics calculations suggest that the formation mechanism of the hydrogen molecules via the Rydberg state are different from that via the vertical electron capture to the ground state of H_4.

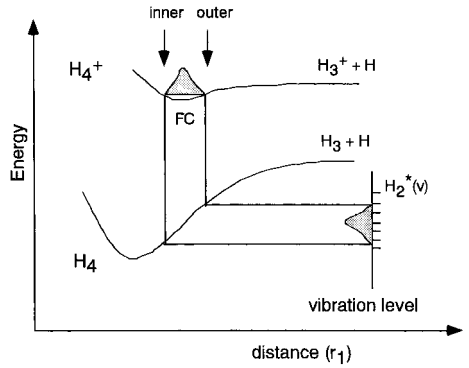

Figure 7. Schematic illustration of the reaction model for the electron capture processes of H_4^+.

4. Discussion

Reaction Model. The reaction model for the electron capture by H_4^+ is illustrated schematically in Figure 7. Lower and upper curves indicate schematically potential energy curves (PECs) for H_4 and H_4^+ along r_1, respectively. The PEC for H_4^+ shows that the hydrogen atom is bound weakly to H_3^+, so that H_4^+ has a wide FC region for the electron capture. In the H_4 system, the H(1) is bound strongly to H(2), so that the PEC for H_4 has a deep basin. Once electron capture occurs, the PEC is changed from H_4^+ to the neutral system H_4. H(1) rapidly approaches H(2), and the H_2 molecule is formed. If electron capture occurs from the outer edge of the FC region (large r_1 distance), the H−H stretching mode of H_2 is highly excited. On the other hand, the electron capture from the inner edge of the FC region leads to H_2 at the lower vibrational state. Thus, the wide FC region gives the wide distribution of vibrational state of hot-H_2. The vibrational mode of the hydrogen molecule H(3)−H(4) is perpendicular to that of H(1)−H(2), so that the intermolecular vibrational energy transfer does not take place, meaning that the vibrational mode of H(3)−H(4) is in the ground state after the electron capture.

In the present study, in addition to the FC region for the r_1-direction, we considered FC region for ϕ-direction as shown in section 3D. The calculations from the outer edge of the FC region ($\phi = 175°$) gave similar results: the hydrogen molecules are composed of hot-H_2 and cold-H_2. The vibrational levels of two hydrogen molecules are $v = 0$ and $v = 7$, and the rotational energies of the hydrogen molecules are in the ground states, although these increase slightly with increasing angle ϕ.

Therefore, it is concluded that the ν_6 mode of H_4^+ is dominant in the reaction dynamics in the electron capture process of H_4^+.

Comparison with the Previous Studies. The feature of the product vibrational and rotational states of H_2 obtained from the present dynamics calculations is in good agreement with that predicted by Pan and Borkman using static ab initio MO calculations.[14] The present calculations strongly support the model proposed by them. However, the feature of the dynamics calculations was modified slightly by the present calculations; the vibrational states of hot-H_2 are widely distributed, because the electron capture occurs from wide the FC region. In addition, we predicted that about 30% of the total available energy is partitioned into the relative translational mode between the hydrogen molecules.

Recently, Nelson et al. calculated energies of the Rydberg states of the meta-stable H_4 cluster using Koopman's theorem at the equilibrium point of H_4^+.[14b] They suggested that the recoil energy between the hydrogen molecules is reduced due to radiative transitions among the Rydberg states, if the Rydberg states are involved in the charge-neutralization process. In the present calculations, the dynamics at the Rydberg states of H_4 were not included, but the ground state of H_4 only was considered. It should be noted therefore that the present model is limited in the ground-state dynamics. Preliminary trajectory calculations from the geometrical conformation at the lowest Rydberg state suggested that the product hydrogen molecules via Rydberg state are different from those of vertical electron capture to the ground state. The dynamics calculations including Rydberg states would be required to solve the complete dynamics of H_4.

Concluding Remarks. We have introduced several approximations to calculate the potential energy surface and to treat the reaction dynamics. First, we assumed that H_4 has no excess energy at the initial step of the trajectory calculation (time = 0.0 ps). This may cause slight change of lifetime and energy distribution of the hydrogen molecules. In higher excess energy, the population of the vibrational quantum number may be shifted to a higher energy region.

Second, we assumed HF/6-311G(d,p) multidimensional potential energy surface in the trajectory calculations throughout. Ab initio MO calculations indicate that the reaction energy (i.e., energy difference between $[H_4]_{ver}$ and $H_2 + H_2$) is calculated to be 5.57 eV at the HF/6-311G(d,p) level. This energy is close to that of the MP4SDQ calculation (5.41 eV). Also, the shape of the potential energy surface around the reaction coordinate calculated at the HF level is similar to that of the MP4SDQ calculation and more accurate surfaces calculated by several groups.[25,26] Therefore, the HF/6-311G(d,p) level of theory would be adequate to discuss qualitatively the dynamics of electron capture by H_4^+. Despite the several assumptions introduced here, the results enable us to obtain valuable information on the mechanism of the electron capture by H_4^+.

Acknowledgment. The author is indebted to the Computer Center at the Institute for Molecular Science (IMS) for the use of the computing facilities. The author acknowledges partial support from a Grant-in-Aid from the Ministry of Education, Science, Sports and Culture of Japan.

References and Notes

(1) Geballe, T. R.; Oka, T. *Nature* **1996**, *384*, 334.
(2) Bawendi, M. G.; Rehfuss, B. D.; Oka, T. *J. Chem. Phys.* **1990**, *93*, 6200.
(3) Carrington A.; West, Y. D.; McNab, I. R. *J. Chem. Phys*. **1993**, *98*, 1073.
(4) Uy, D.; Gabrys, C. M.; Jagod, M. F.; Oka, T. *J. Chem. Phys*. **1994**, *100*, 6267.
(5) Lie, G. C.; Frye, D. *J. Chem. Phys.* **1992**, *96*, 6784.
(6) Henderson, J. R.; Tennyson, J.; Sutcliffe, B. T. *J. Chem. Phys*. **1993**, *98*, 7191.
(7) Carter, S.; Meyer, W. *J. Chem. Phys.* **1994**, *100*, 2104.
(8) Bramley, M. J.; Tromp, J. W.; Carrington, T.; Corey, G. C. *J. Chem. Phys.* **1994**, *100*, 6175.
(9) Ignacio, E. W.; Yamabe, S. *Chem. Phys. Lett*. **1998**, *287*, 563.
(10) Paul, W.; Lucke, B.; Schlemmer, S.; Gerlich, D. *Int. J. Mass Spectrom. Ion Processes* **1995**, *149*, 373.
(11) Paul, W.; Schlemmer, S.; Lucke, B.; Gerlich, D. *Chem. Phys.* **1996**, *209*, 265.
(12) Jungwirth, P.; Carsky, P.; Bally, T. *Chem. Phys. Lett.* **1992**, *195*, 371.
(13) Alvarez-Collado, R. J.; Aguado, A.; Paniagua, M. *J. Phys. Chem*. **1995**, *102*, 5725.
(14) (a) Pan, Z.; Borkman, R. F. *J. Phys. Chem.* **1995**, *99*, 916. (b) Nelson, M. R.; Cobb, M. G.; Borkman, R. F. *J. Phys. Chem.* **1997**, *101*, 8932.
(15) (a) Kirchner, N. J.; Gilbert, J. R.; Bowers, M. T. *Chem. Phys. Lett*. **1984**, *106*, 7. (b) Kirchner, N. J.; Bowers, M. T. *J. Chem. Phys*. **1987**, *86*, 1301.
(16) Borkman, R. F.; Cobb, M. *J. Chem. Phys.* **1981**, *74*, 2920.
(17) Wright, L. R.; Borkman, R. F. *J. Chem. Phys*. **1982**, *77*, 1938.
(18) Cardeline, B. H.; Eberhardt, W. H.; Borkman, R. F. *J. Chem. Phys*. **1986**, *84*, 3230.
(19) Figureger, H.; Ketterle, W.; Walther, H. *Z. Phys. D At. Mol. Clusters* **1989**, *13*, 129.
(20) Ketterle, W.; Figureger, H.; Walther, H. *Z. Phys. D At. Mol. Clusters* **1989**, *13*, 139.
(21) Karplus, M.; Porter, R. N.; Sharm, R. D. *J. Chem. Phys.* **1965**, *43*, 3259.
(22) (a) Tachikawa, H. *J. Chem. Phys*. **1998**, *108*, 3966. (b) Tachikawa, H. *J. Phys. B* **1999**, *32*, 1451. (c) Tachikawa, H. *J. Phys. Chem.* **1995**, *99*, 225. (d) For a review article, Tachikawa, H. *Trends Phys. Chem.* **1997**, *6*, 279.
(23) (a) Tachikawa, H. *J. Phys. Chem. A* **1998**, *102*, 7065. (b) Tachikawa, H.; Igarashi, M. *J. Phys. Chem. A* **1998**, *102*, 8648. (c) Tachikawa, H. *J. Phys. Chem. A* **1997**, *101*, 7475. (d) Tachikawa, H. *J. Phys. Chem. A* **1999**, *103*, 6873. (e) Tachikawa, H. *Phys. Chem. Chem. Phys.* **1999**, *1*, 2675. (f) Tachikawa, H. *Phys. Chem. Chem. Phys.* **1999**, *1*, 4925. (g) Program code of the direct ab initio dynamics calculation was created by our group.
(24) Ab initio MO calculation program, *Gaussian 94*: Frisch, M. J.; Trucks, G. W.; Schlegel, H. B.; Gill, P. M. W.; Johnson, B. G.; Robb, M. A.; Cheeseman; J. R.; Keith, T.; Petersson, G. A.; Montgomery, J. A.; Raghavachari, K.; Al-Laham, M. A.; Zakrzewski, V. G.; Ortiz, J. V.; Foresman, J. B.; Cioslowski, J.; Stefanov, B. B.; Nanayakkara, A.; Challacombe, M.; Peng, C. Y.; Ayala, P. Y.; Chen, W.; Wong, M. W.; Andres, J. L.; Replogle, E. S.; Gomperts, R.; Martin, R. L.; Fox, D. J.; Binkley, J. S.; Defrees, D. J.; Baker, J.; Stewart, J. P.; Head-Gordon, M.; Gonzalez, C.; Pople, J. A. *Gaussian 94, Revision D.3*; Gaussian, Inc.: Pittsburgh, PA, 1995.
(25) Ceballos, A.; Garcia, E.; Rodriguez, A.; Lagana, A. *Chem. Phys. Lett.* **1999**, 276.
(26) Boothroyd, A.; Dove, J. E.; Keogh, W. J.; Martin, P. G.; Peterson, M. R. *J. Chem. Phys.* **1991**, *95*, 4331.